

Helium Exhaust Studies in *H*-Mode Discharges in the DIII-D Tokamak Using an Argon-Frosted Divertor Cryopump

M. R. Wade,² D. L. Hillis,² J. T. Hogan,² M. A. Mahdavi,¹ R. Maingi,² W. P. West,¹ N. H. Brooks,¹ K. H. Burrell,¹ R. J. Groebner,¹ G. L. Jackson,¹ C. C. Klepper,² G. Laughon,¹ M. M. Menon,² P. K. Mioduszewski,² and DIII-D Team¹

¹General Atomics, San Diego, California 92184

²Oak Ridge National Laboratory, Oak Ridge, Tennessee 37831

(Received 26 April 1994)

The first experiments demonstrating exhaust of thermal helium in a diverted, *H*-mode deuterium plasma have been performed on the DIII-D tokamak. The helium, introduced via gas puffing, is observed to reach the plasma core, and then is readily removed from the plasma with a time constant of ~ 10 – 20 energy-confinement times by an in-vessel cryopump conditioned with argon frosting. Detailed analysis of the helium profile evolution suggests that the exhaust rate is limited by the exhaust efficiency of the pump ($\sim 5\%$) and not by the intrinsic helium-transport properties of the plasma.

PACS numbers: 52.55.Fa

In future burning-fusion devices based on the deuterium-tritium (D-T) reaction, the “ash” of such reactions, helium (He), will be an unavoidable impurity component of the plasma. The overall performance of such devices is critically dependent on the ability to efficiently and continuously remove this He ash from the plasma core to prevent dilution of the D-T fuel. Such dilution manifests itself in degradation of reactor performance and, if severe enough, could cause quenching of the thermonuclear burn. The attractiveness of a particular operating scenario is therefore inherently dependent not only on the thermal confinement properties of that regime but also on the He exhaust capabilities. In this regard, there are two primary energy-confinement regimes in which steady-state operation has been reliably achieved on present-day devices, the low-confinement mode (*L* mode) and the high-confinement mode (*H* mode) with edge-localized modes (ELM's). Previous studies on several tokamak devices have demonstrated that sufficient He exhaust can be obtained in plasmas with *L*-mode confinement characteristics [1–5]. However, in terms of energy confinement, heat removal, and particle handling characteristics, the most promising, steady-state operation regime obtained to date is *H* mode in a diverted, magnetic configuration. A long-standing objection to the *H*-mode regime has been the possibility that particle (and hence ash) removal would be insufficient. To date, helium exhaust measurements in *H* mode have been limited to polarization-induced, quiescent *H*-mode plasmas in TEXTOR, a limiter device, and have produced unfavorable results in terms of He exhaust [6]. In this Letter, we report recent experimental results from the DIII-D tokamak in which significant He exhaust in diverted, *H*-mode plasmas has been demonstrated for the first time.

In judging He exhaust capabilities, the figure of merit generally used is the ratio of the global residence time of the He ash within the plasma chamber τ_{He}^* to the plasma energy-confinement time τ_E . Studies have shown that successful operation of a reactor can be maintained

only if the He ash is removed from the system within 7–15 energy-confinement times (i.e., $\tau_{\text{He}}^*/\tau_E \leq 7$ – 15), depending on the impurity content of the plasma [7]. If $\tau_{\text{He}}^*/\tau_E$ exceeds this value, significant fuel dilution will occur and could cause eventual quenching of the thermonuclear burn. In the experiments discussed here, $\tau_{\text{He}}^*/\tau_E \sim 10$ has been achieved in an *H*-mode plasma simultaneously with good energy confinement. This result is a clear demonstration that the He exhaust rate of a high-confinement, *H*-mode plasma should be sufficient for a reactor.

This experimental study was made possible by the recent installation of a cryocondensation pump as part of an advanced divertor configuration on DIII-D [8–10]. Figure 1 shows a cross section of the lower divertor of DIII-D and the associated hardware. The divertor hardware consists of a toroidally continuous baffle plate, bias ring, and cryocondensation pump. The baffle plate forms a pumping plenum, which is closely coupled to the divertor plasma when the outer strike point (OSP) is located near the baffle entrance. The pump is located inside the pumping plenum defined by the baffle plate and consists of a liquid-helium (LHe) cooled pumping surface that is surrounded by a liquid-nitrogen cooled shield. The pump has a measured pumping speed for deuterium of approximately 30 000 l/s [11]. Through the use of this pump, density control in *H*-mode plasmas has been demonstrated with steady-state densities obtained that are $\sim 50\%$ lower than those obtained without active pumping [12]. To facilitate the pumping of He, an argon (Ar) frost layer was condensed on the LHe surface of the cryopump between successive plasma discharges by isolating the vacuum chamber from the external turbomolecular pumps and injecting a known amount of Ar into the main vacuum chamber. In this manner, a layer of ~ 1500 torr \cdot l (~ 1.5 μm thick layer) was condensed on the pump, providing a measured pumping speed for He of approximately 18 000 l/s when the layer is fresh. It should be noted that deuterium is also pumped via the Ar frost and that the pumping speed for He decreases

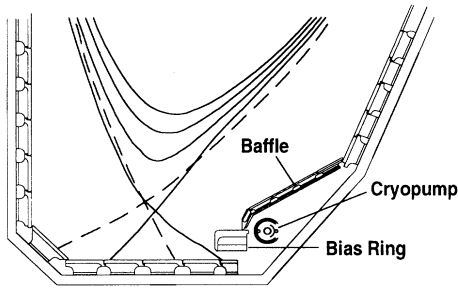


FIG. 1. Schematic of the lower divertor of DIII-D showing the location of the baffle plate, bias ring, and cryocondensation pump. Also shown are magnetic equilibria with the outer strike point (OSP) close to the pumping plenum entrance (solid lines) and with the OSP far away from the entrance (dashed lines).

substantially as the amount of deuterium absorbed on the pump increases.

To simulate the presence of He ash in these experiments, a short (50 ms) puff of He gas is injected and allowed to diffuse into the plasma core. Sufficient He is introduced to bring the He concentration to $\sim 15\%$ of the electron density n_e . A set of spectroscopic diagnostics is used to follow the evolution of He in the plasma core, divertor, and pumping plenum. The evolution of the He density profile in the plasma core is measured with a high resolution spectroscopy system, which uses the techniques of active charge-exchange recombination (CER) spectroscopy. The DIII-D CER system has 32 channels that span the entire cross section with excellent spatial resolution over the entire profile (3 cm in the core, 3 mm at the edge) [13]. The He density profile is inferred from measurements of the intensities of the He II $n = 4-3$ transition at 4685.68 \AA induced by charge-exchange excitation. Modulation of the neutral beams at a frequency of 100 Hz was used to simplify computational analysis of the measured CER spectra. A modified Penning gauge, located in an appendage to the pumping plenum, is used to measure the He and deuterium partial pressure [14]. The time response of this gauge is approximately 50 ms.

Because the He is introduced at the plasma edge, the evolution of the He density within the plasma core is strongly dependent on the He exhaust rate. Therefore, the sequencing of this experiment is critical to allow the He introduced at the edge to evolve to the plasma core before strong pumping is applied. Previous measurements have shown that large pressures are obtained in the pumping plenum of DIII-D only when the gap between the divertor's outer strike point and the bias ring Δ_{OSP} is less than 4 cm [15]. Taking advantage of the fact that the effective He exhaust rate is the product of the cryopump pumping speed and the partial pressure of He in the baffle region, the exhaust rate is regulated in this experiment by controlling the position of the OSP. From the initiation of the discharge until well after the He gas puff, the OSP is maintained well away from the baffle entrance ($\Delta_{OSP} \sim 15 \text{ cm}$). A representative magnetic equilibrium

reconstructed from external magnetic measurements by the EFITD code [16] is shown as the dashed lines in Fig. 1. After the He density profile has come to steady state subsequent to the He gas puff, strong He exhaust is initiated by rapidly moving the OSP to the throat of the baffle entrance ($\Delta_{OSP} = 1.5 \text{ cm}$). The OSP is then maintained in this location for the remainder of the discharge so as to provide maximum exhaust efficiency. A representative magnetic equilibrium for times subsequent to the OSP sweep is shown as the solid lines in Fig. 1.

The temporal evolution of a typical He exhaust discharge is shown in Fig. 2. For the experiments discussed here, a lower, single-null, divertor configuration was used with a plasma current of 1.0 MA and a major radius of $\sim 1.67 \text{ m}$. A steady neutral beam power of 4.2 MW was applied throughout the discharge. The $L-H$ mode transition occurs at $\sim 1.25 \text{ s}$ in this discharge as evidenced by the rapid drop in D_α radiation and increase in plasma density and temperature. The He gas puff ($\sim 6.0 \text{ Torr l total}$, 50 ms duration) is introduced at 1.5 s, and the OSP sweep to the baffle entrance described above is performed at 2.0 s. Following a short ELM-free period, type-I ELMs [17] begin and continue with an average frequency of $\sim 200 \text{ Hz}$ until the OSP sweep when the ELM frequency decreases to $\sim 20 \text{ Hz}$. This decrease is most likely due to a reduction in the edge pressure gradient as a result of pumping, which in turn changes the stability characteristics of the edge. Deuterium gas puffing was disabled during the H -mode portion of this discharge; hence,

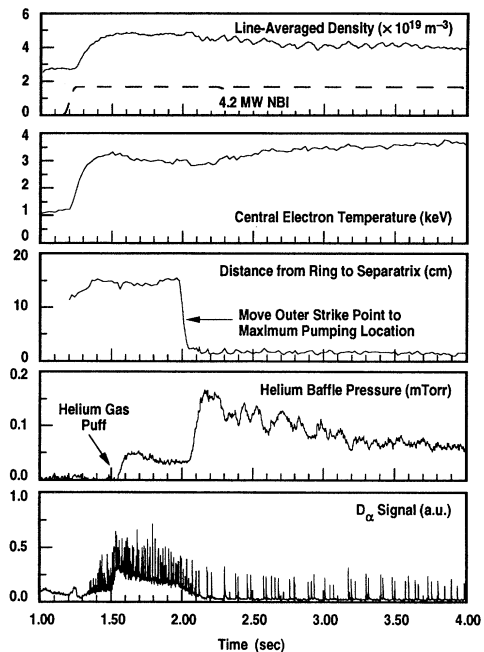


FIG. 2. Time evolution of the line-averaged n_e , central electron temperature, the closest approach of the outer divertor leg to the bias ring Δ_{OSP} , the helium partial pressure in the pumping plenum, and the divertor D_α radiation in a discharge with active helium exhaust and $P_{NBI} = 4.2 \text{ MW}$.

the line-averaged n_e decreases slightly due to pumping from $6.4 \times 10^{19} \text{ m}^{-3}$ at the time of the OSP sweep to $5.2 \times 10^{19} \text{ m}^{-3}$ at 3.9 s. There is a corresponding increase of the electron and ion temperature from 2.8 to 3.4 keV. No evidence of Ar evolving from the pump to the plasma core was observed by either vacuum ultraviolet (vuv) spectroscopy or soft x-ray emission.

The temporal evolution of the He density near the plasma center (normalized radius $\rho = 0.3$) is shown in Fig. 3 for discharges with and without Ar frost applied to the cryopump. Note that the pump is exhausting deuterium in both of these discharges since the cryopanel is at LHe temperature in both cases; hence, the evolution of the background plasma is essentially the same. The evolution of the He density is observed to be roughly the same in both cases until the OSP is swept to the baffle entrance at 2.0 s. The core He density rises sharply just after the He gas puff and reaches steady state in the plasma core after ~ 200 ms. In steady state with no Ar applied to the pump, both the He concentration (relative to n_e) in the plasma core and the He atomic fraction in the pumping plenum is $\sim 15\%$. In addition, the core He density remains approximately constant after the initial rise, although a small decrease in the He density is observed at the time of the OSP sweep. The magnitude of this decrease is consistent with a simultaneous increase of He partial pressure in the pumping plenum, suggesting that the observed decrease is due to a "baffling" effect in which a significant amount of He is being retained within the pumping plenum volume without actually being exhausted from the system.

With Ar frost applied to the pump, the He density decreases rapidly starting at 2.0 s with approximately 65%

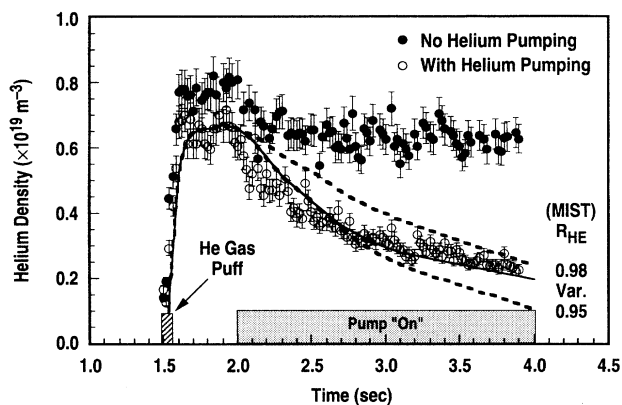


FIG. 3. Comparison of the evolution of the helium density near the plasma center measured with CER spectroscopy during discharges with and without Ar frost applied to the divertor cryopump. Helium was puffed at 1.5 s, and the divertor OSP was swept to the baffle entrance at 2.0 s to initiate active pumping. The dashed curves represent MIST transport calculations using different recycling models after the OSP sweep: (a) $R_{\text{He}} = 0.98$, (b) steadily increasing R_{He} with $R_{\text{He}} = 0.95$ at the OSP sweep, (c) $R_{\text{He}} = 0.95$. R_{He} is assumed to be unity before the OSP.

of the He being exhausted within 2.0 s. From CER measurements, the time dependence of the total plasma inventory of He ions can be determined and should be consistent with the He global particle balance equation $dN_{\text{He}}/dt = -N_{\text{He}}/\tau_{\text{He}} + R_{\text{He}}N_{\text{He}}/\tau_{\text{He}} + S_{\text{He}}$, where N_{He} is the total number of He ions in the plasma, τ_{He} is the He particle confinement time, R_{He} is the He recycling coefficient, and S_{He} is the external He particle source rate. In this experiment, $S_{\text{He}} = 0$ after the initial He gas puff. This equation can be further simplified by defining $\tau_{\text{He}}^* = \tau_{\text{He}}/(1 - R_{\text{He}}) = \tau_{\text{He}}/\mathcal{E}_{\text{He}}$, where \mathcal{E}_{He} is the exhaust efficiency of the pumping system. In a case in which R_{He} is constant, the e -folding time of the total He inventory in the plasma is τ_{He}^* . In the discharge of interest, this characteristic time constant is found to be $\tau_{\text{He}}^* = 2.20$ s. Using measured profiles of electron density and temperature, ion temperature, and Z_{eff} , the plasma stored energy can be readily calculated and is found to be 0.58 MJ, which yields $\tau_E = 137$ ms. This energy confinement time is consistent with the JET/DIII-D ELM-free H -mode database scaling [18]. With this information, the ratio $\tau_{\text{He}}^*/\tau_E$ is found to be ~ 16 . However, because of reasons to be discussed later, the exhaust efficiency is not constant, and this value is an overestimate of $\tau_{\text{He}}^*/\tau_E$ for this discharge.

As mentioned earlier, nonplasma tests on DIII-D of the pumping speed of the Ar frost layer on the cryopump have shown a pronounced degradation of the pumping speed for He as the amount of deuterium absorbed on the Ar frost is increased [19]. These tests have shown that the pumping speed for He decreases roughly exponentially with deuterium loading from ~ 18000 l/s when the Ar frost is fresh (i.e., no deuterium loading) to ~ 7000 l/s with ~ 100 Torr l deuterium absorbed within the Ar frost layer. In the discharge of interest, this translates into a decrease in pumping speed from ~ 14000 l/s (~ 25 Torr l D_2 absorbed on pump) at the initiation of active pumping to ~ 8100 l/s (~ 80 Torr l absorbed on pump) at the end of the pump-out phase ($t = 4.0$ s). The primary effect of this variation in pumping speed is that the exhaust efficiency \mathcal{E}_{He} is not constant throughout the discharge. The time dependence of this reduction can be taken into account by assuming $\mathcal{E}_{\text{He}}(t) = \mathcal{E}_{\text{He},0}(1 - \alpha t)$. In this case, the minimum obtainable τ_{He}^* is $\tau_{\text{He},\text{min}}^* = \tau_{\text{He}}/\mathcal{E}_{\text{He},0}$. The parameter α can be estimated from the pumping speed falloff as outlined above and yields $\alpha = 0.21$. Using this value, $\tau_{\text{He},\text{min}}^*$ is found to be ~ 1.44 s and $\tau_{\text{He}}^*/\tau_E \sim 10$. Because the time history of the actual pumping speed in the discharge of interest was not measured and is difficult to estimate, it is also instructive to let α be a free parameter in fitting the measured He density evolution. When this is done, $\alpha \sim 0.45$, $\tau_{\text{He},\text{min}}^* \sim 1.11$ s and $\tau_{\text{He}}^*/\tau_E \sim 8$. Either of these results is within the range generally considered necessary for successful operation of future reactors, such as ITER.

Detailed measurements of the He density profile during this active exhaust phase indicate that the He density profile shape remains essentially unchanged as is shown

in Fig. 4. This observation coupled with the fact that the He density at $\rho = 0.3$ responds within ~ 20 ms to the initiation of active pumping suggests that the exhaust of He is limited by the effective exhaust efficiency of the pumping configuration and not by transport of He within the plasma core.

The measured He density profiles have been modeled also with the MIST impurity transport code [20]. MIST uses the experimentally measured n_e and T_e profiles as a function of radius and time as input. The code computes the He density profiles as a function of time given a spatially dependent anomalous diffusivity D_{He} , a pinch velocity [$n_e V_{\text{He}} = C_v D_{\text{He}} dn_e/dr$], and a global He recycling coefficient R_{He} . As with prior fits to DIII-D H-mode data, [20], it is assumed that the pinch coefficient C_v is unity, based on the close agreement between the electron and He density profile shapes in steady state. For the discharge of interest, the best fit is obtained with a time-dependent recycling model and a diffusivity coefficient that has the approximate form $D_{\text{He}} = 0.5 \text{ m}^2/\text{s}$ for $\rho < 0.4$, $D_{\text{He}} = 1.75 \text{ m}^2/\text{s}$ for $\rho > 0.6$ with a sharp gradient region between $\rho = 0.4$ and $\rho = 0.6$. The sensitivity to the recycling model used in the simulation is demonstrated in Fig. 3 where the simulated data are plotted for a fixed $R_{\text{He}} = 0.95$ a fixed $R_{\text{He}} = 0.98$, and a steadily increasing R_{He} with the initial $R_{\text{He}} = 0.95$. In all cases, R_{He} is assumed to be unity before the OSP at 2.0 s. The best fit to the measured data is obtained with a steadily increasing R_{He} with $R_{\text{He}} = 0.95$ just after the initiation of active He exhaust at 2.0 s, providing further evidence that $\tau_{\text{He}} \ll \tau_{\text{He}}^*$.

The results from these experiments indicate that sufficient He exhaust for successful operation of a reactor is achievable in H- and EL-mode conditions in a divertor configuration with an exhaust efficiency of only $\sim 5\%$. Helium exhaust has been measured in several H- and EL-mode discharges in DIII-D, and, in all cases, $\tau_{\text{He}}^*/\tau_E$ has been found to be in the range $10 \leq \tau_{\text{He}}^*/\tau_E \leq 20$, within

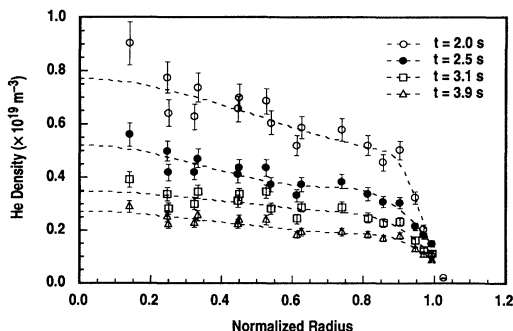


FIG. 4. Helium density profiles as measured by CER spectroscopy at various times during a discharge with active helium exhaust. Active helium exhaust is initiated at $t = 2.0$ s via a sweep of the divertor OSP. The dashed lines are spline fits to the measured data.

the acceptable range for reactors. Since ELMs have been shown to enhance transport of impurities, including He, in the plasma edge in previous studies [6,21–23] one can expect an even lower value for $\tau_{\text{He}}^*/\tau_E$ at higher ELM frequencies.

We gratefully acknowledge the assistance of D. Finkelenthal, P. Gohil, and R. Seraydarian in calibrating the CER system and the contributions of the DIII-D operations staff. This research was sponsored by the U.S. Department of Energy, under Contracts No. DE-AC05-84OR21400 with Martin Marietta Energy Systems, Inc. and No. DE-AC03-89ER51114 with General Atomics and by an appointment in the Magnetic Fusion Energy Postdoctoral Program, administered by Oak Ridge Associated Universities.

- [1] D.L. Hillis *et al.*, Phys. Rev. Lett. **65**, 2382 (1990).
- [2] D.L. Hillis *et al.*, in *Proceedings of the Thirtieth International Conference on Plasma Physics and Nuclear Fusion Research, Washington, 1990* (International Atomic Energy Agency, Vienna, 1991), Vol. 3, p. 597.
- [3] E.J. Synakowski *et al.*, Phys. Rev. Lett. **65**, 2255 (1990).
- [4] H. Nakamura *et al.*, Phys. Rev. Lett. **67**, 2658 (1991).
- [5] E.J. Synakowski *et al.*, Phys. Fluids B **5**, 2215 (1993).
- [6] D.L. Hillis *et al.*, J. Nucl. Mater. **196-198**, 35 (1992).
- [7] D. Reiter *et al.*, Nucl. Fusion **30**, 2141 (1990).
- [8] M.M. Menon *et al.*, Fusion Tech. **22**, 356 (1992).
- [9] J.P. Smith *et al.*, in *Proceedings of the 15th IEEE/NPSS Symposium on Fusion Engineering, Hyannis, 1993* (IEEE, Piscataway, 1994), Vol. 2, p. 1043.
- [10] K. Schaubel *et al.*, Adv. Cryogenic Eng. **39**, 1583 (1994).
- [11] M.M. Menon *et al.*, in *Proceedings of the 15th IEEE/NPSS Symposium on Fusion Engineering, Hyannis, 1993* (IEEE, Piscataway, 1994), Vol. 2, p. 1047.
- [12] M.A. Mahdavi *et al.*, in *Proceedings of the 20th EPS Conference on Controlled Fusion and Plasma Physics, Lisbon, 1993* (European Physical Society, Petit-Lancy, 1993), Vol. 17C, Part II, p. 647.
- [13] P. Gohil *et al.*, in *Proceedings of the 14th Symposium on Fusion Engineering, San Diego, 1992* (IEEE, Piscataway, 1992), Vol. 2, p. 1199.
- [14] K.H. Finken *et al.*, Rev. Sci. Instrum. **63**, 1 (1992).
- [15] C.C. Klepper *et al.*, Nucl. Fusion **33**, 533 (1993).
- [16] L.L. Lao *et al.*, Nucl. Fusion **30**, 1035 (1990).
- [17] E.J. Doyle *et al.*, Phys. Fluids B **3**, 2300 (1991).
- [18] D.P. Schissel *et al.*, Nucl. Fusion **31**, 73 (1991).
- [19] M.M. Menon (private communication).
- [20] R.A. Hulse, Nucl. Technol. Fusion **3**, 259 (1983).
- [21] M.R. Wade, in *Proceedings of the 20th EPS Conference on Controlled Fusion and Plasma Physics, Lisbon, 1993*, [12], Vol. 17C, Part I, p. 63.
- [22] M.A. Mahdavi *et al.*, in *Proceedings of the 16th EPS Conference on Controlled Fusion and Plasma Physics, Venice, 1989* (European Physical Society, Petit-Lancy, 1993), Vol. 13B, Part I, p. 249.
- [23] M.E. Perry *et al.*, Nucl. Fusion **31**, 1991 (1991).